Catalysis Science & Technology

Accepted Manuscript

ROYAL SOCIETY OF CHEMISTRY

www.rsc.org/catalysis

Hydrochlorination of acetylene using supported phosphorus doped Cu-based catalysts

Hang Li, Fumin Wang, Wangfeng Cai, Jinli Zhang, Xubin Zhang*[a]

Phosphorus-doped copper catalysts supported on spherical activated carbon（SAC） were prepared using an incipient wetness impregnation technique. The catalysts were characterized by low-temperature N_2 adsorption/desorption, X-ray diffraction (XRD), transmission electron microscopy (TEM), temperature programmed reduction (TPR), X-ray photoelectron spectroscopy (XPS), inductively coupled plasma (ICP), N_2O pulse titration method and thermogravimetric (TG) technologies. The results indicate that the phosphorus-doped Cu-based catalysts exhibit both high activity and good stability. The amount of phosphorus dopant has a significant effect on the catalytic activity of acetylene hydrochlorination and the optimal molar ratio of Cu/P is 2.5. The phosphorus doping facilitates the dispersion of copper species, enhances the interaction between metal and support, and restrains the growth of copper species during acetylene hydrochlorination. These results suggest that this high-activity, good-stability and low-cost catalyst has a great potential in industrial applications.

[a]*School of Chemical Engineering & Technology, Tianjin University, Tianjin 300072, People's Republic of China. Fax: +86-022-2789-0041; Tel: +86-022-2789-0041; E-mail: tjzxb@tju.edu.cn*

Introduction

Acetylene hydrochlorination is currently an important industrial process used to manufacture vinyl chloride, which is the monomer used to synthesize polyvinyl chloride (PVC).[1] There are two main methods for synthesis of VCM, acetylene hydrochlorination and ethylene oxychlorination respectively. Ethylene-based processes are widely used in many developed countries, but acetylene hydrochlorination is more preferable in locations where coal resources are relatively rich.[1-3] To date, activated-carbon-supported mercuric chloride ($HgCl_2$/C) catalysts were most widely applied in acetylene hydrochlorination.[4] But, mercury is highly toxic and volatile and may cause serious harm to both workers and the environment.[5-7] Therefore, it is imperative to find alternatives for mercuric catalysts during acetylene hydrochlorination to promote the sustainable development of PVC production.

In recent years, many metal catalysts have been used as substitutes for the toxic mercuric catalysts. Hutchings *et al*. used more than 20 types of metal components for acetylene hydrochlorination and found that the catalytic activity was associated with the standard electrode potential of the metal cations. The order of initial activity was Pd^{2+} > Hg^{2+} > Cu^{2+}, Cu^{+} > Ag^{+}.[8-14] Later, the researchers fully studied carbon-supported gold catalysts and found that Au/C had a high catalytic activity. However, noble metal catalysts usually suffer from disadvantages related to high cost and rapidly deactivation due to coke deposition or the reduction of metal cations.[15] Thus, the development of low cost, environmentally benign, sustainable catalysts is

becoming urgent. It is known that Cu-based catalysts have been intensively investigated due to its higher activity for vapor-phase hydrogenation reaction.[16] Similarly, Cu-based catalysts as an alternative can also have good activity in acetylene hydrochlorination. Zhou,[17] for example, studied the copper chlorides NPs loaded on the nitrogen-doped carbon nanotubes (N-CNTs) for acetylene hydrochlorination and concluded that the Cu-NCNT catalyst (2.4% N) offers promoted reactivity for sustainable hydrochlorination. But, it still remains unclear what role the copper species play in the acetylene hydrochlorination reaction and in the deactivation mechanism of Cu-based catalysts, thus it is needed to be further studied.

As we all know, dopants of non-metal elements like nitrogen, boron and phosphorus on carbon material can improve the performance of the catalysts for the oxygen reduction reaction.[18-21] Peng and co-workers[22, 23] prepared P-doped graphitic layers and carbon nanotubes to show high ORR performance and they found that phosphorus dopant can change the electronical structure in the network of graphitic layers so as to improve the electrocatalytic activity of catalysts. Cheng[24] found that the ORR activity can be improved owing to the formation of more structural defects after inducing phosphorus. Yang[25] reported that phosphorus doping on the standard Fe-N/C ORR catalyst exhibited a much enhanced ORR performance and the phosphorus doping process might not alter the nature of active sites but lead to the increase of ORR active site density and better dispersion of them on the catalyst surface. However, whether the P-dopant can improve the activity and the stability of

Cu-based catalysts for acetylene hydrochlorination is still unknown.

In this paper, a series of phosphorus-modified carbon-supported copper catalysts were prepared using phosphoric acid as the phosphorus source. Catalytic activity and stability of phosphorus doped catalysts for acetylene hydrochlorination were investigated. Besides, the influence of phosphorus doping on the structure of the catalysts was also deeply discussed and recognized.

Experimental

Catalyst preparation

The carbon-supported copper catalysts were prepared using an incipient wetness impregnation technique with distilled water as a solvent. The spherical activated carbon (SAC0609, 18-28 mesh) was initially washed with dilute aqueous HCl ($1 mol \cdot L^{-1}$) at 80 ℃ for 5 h to remove the poisonous components, such as Na, Fe contaminants. The carbon support was filtered and washed with distilled water, and then dried at 120 ℃ for 18 h. The pretreated carbon (5.0 g) was added to a solution of $CuCl_2 \cdot 2H_2O$ (A.R.) (5 mL) and maintained at 80 ℃ for 12 h. The catalysts were dried at 120 ℃ for 12 h, and then calcined from room temperature to 500 ℃ at a heating ramp of 10 ℃·min and a dwell time of 5 h under nitrogen flow. The obtained catalysts were named Cu/SAC.

Phosphoric acid-modified Cu/SAC catalysts were prepared by an impregnation method by immersing the calcined Cu/SAC in a phosphoric acid solution, then stirred for 4 h, subsequently dried at 120 ℃ for 12 h and calcined in nitrogen (500 ℃, 5 h). The calcined sample was designed as xCuP/SAC, where x represents the molar ratio

of Cu/P.

The carbon-supported cupric pyrophosphate catalyst was also prepared using an incipient wetness impregnation technique. The pretreated carbon (5.0 g) was added to a solution of $Cu_2P_2O_7$ (A.R.) (5 mL) and maintained at 80 ºC for 12 h. The catalysts were dried at 120 ℃ for 12 h, and then calcined from room temperature to 500 ℃ at a heating ramp of 10 ℃·min and a dwell time of 5 h under nitrogen flow. The obtained catalysts were named $Cu_2P_2O_7$/SAC.

Catalyst performance testing

In order to test the activity of the catalyst, the catalytic performance tests were carried out in a set of tubular fixed-bed microreactor (i.d. 10 mm). The reactor was flushed using nitrogen in order to get rid of water vapor and air. And then the clean HCl and C_2H_2 were fed into the reactor containing 5mL catalysts, and the flowrates were controlled via calibrated mass flow controllers to get a volume ratio HCl: C_2H_2 of 1.15:1 and a C_2H_2 gas hourly space velocity (GHSV) of 180 h^{-1}.The reaction conditions were maintained at 140 ºC, atmospheric pressure. The effluent streams of the reactor were absorbed by NaOH aqueous solution and then analyzed using a Beifen 3420A gas chromatograph equipped with a hydrogen flame inonization detector (FID).

Catalyst characterization

Textual properties of the samples were determined by a nitrogen adsorption method using a CHEMBET-3000 instrument at 77 K. Pore size distribution was calculated by DFT method, and the specific surface areas were calculated from the isotherms using

the BET method. The range of relative pressure of nitrogen was between 0.05 and 0.2.

The X-ray diffraction (XRD) patterns were collected on a Bruker AXS D8 Advance X-ray diffractometor using Cu-K_a radiation (λ=0.15418 nm) in the 2θ scan range from 10° to 80°. Transmission electron microscopy (TEM) was performed on a JEM-2010FEF instrument. The catalyst samples were crushed into powder, and dispersed in ethanol, and then, droplets of the suspension were laid and vaporized on a 300-mesh copper TEM grid with a holey carbon film. Temperature programmed reduction (TPR) instrument was carried out in a micro-flow reactor. For each experiment, a catalyst sample (100mg) was heated from 50 ºC to 850 ºC with a rate of 10 ºC·min^{-1} fed with a 20 mL·min^{-1} nitrogen gas containing 5 vol% H_2.

The dispersion of surface copper was measured by the adsorption and decomposition of N_2O using the pulse titration method.[26]

X-Ray photoelectron spectroscopy (XPS) spectra were recorded using a Kratos Axis Ultra DLD spectrometer employing a monochromated Al-K_a X-ray source (hv = 1486.6 eV), hybrid (magnetic/electrostatic) optics and a multi-channel plate and delay line detector (DLD). All XPS spectra were recorded using an aperture slot of 300×700 microns, survey spectra recorded with pass energy of 80 eV, and high resolution spectra with pass energy of 40 eV. The total content of Cu in the catalysts was determined by a Thermo Scientific iCAP 6000 inductively coupled plasma-atomic emission spectrometer (ICP-AES). The thermogravimetric analysis (TG) was carried out to detect carbon deposition using a NETZSCH STA 449F3

Jupiter®, under air atmosphere at a flowrate of 20 mL·min^{-1}. The temperature was increased from 50 ℃ to 800 ℃ with a heating rate of 10 ℃·min^{-1}.

Results and discussion

Catalytic performances in acetylene hydrochlorination

In this experiment, the support SAC was fixed while their Cu loadings were varied and the catalytic performance of catalysts were tested under the conditions (temperature (T) = 140 ºC, C_2H_2 gas hourly space velocity (GHSV) = 180 h^{-1}). The correlation between Cu loading and catalytic performance is shown in Fig. 1. The catalysts exhibited good performance, and the C_2H_2 conversion increased with increasing Cu loading and further increasing the Cu loading led to a decrease in conversion of reaction, which may be contributed by the aggregation of the active sites. It is worthwhile to note that the acetylene conversion achieved highest (40.5%) of 15wt% Cu loading. Meantime the selectivity was >99% for all catalysts as listed in Table 1. It can be also observed that the conversions slightly decreased after 500 min reaction for Cu catalysts, meantime the selectivity to VCM still maintains 99% after reaction, indicating Cu/SAC catalysts still behave good stability after 500 min reaction.

Table 1 Hydrochlorination performance of catalysts[a]

Catalyst	S_{VC}/%
4wt% Cu/SAC	99.5
6wt% Cu/SAC	99.7
8wt% Cu/SAC	99.8
10wt% Cu/SAC	99.6
12wt% Cu/SAC	99.8

15wt% Cu/SAC	99.6
18wt% Cu/SAC	99.8
24wt% Cu/SAC	99.6

[a]Reaction conditions: T=140 ºC, n(HCl)/n(C_2H_2) = 1.15, GHSV (C_2H_2)=180 h^{-1}

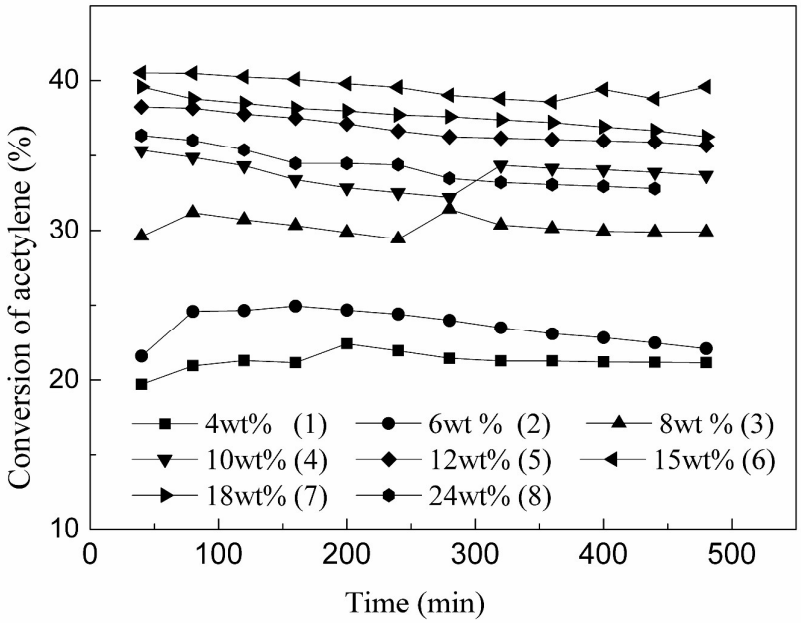

Fig. 1 The relationship between activity and the copper loadings. Reaction conditions: Temperature =140 ºC, GHSV (C_2H_2) = 180 h^{-1}, n(HCl)/n(C_2H_2) = 1.15

We further studied the catalytic performances of Cu-based catalysts with the same support SAC but different phosphorus content doped on the catalysts. Because thermostable cupric pyrophosphate can be formed in the process of preparation, the $Cu_2P_2O_7$/SAC was also prepared for comparison. Given that the optimum loading of copper catalysts has been determined above, the Cu-based catalysts were prepared at loading of 15wt%. Fig. 2 shows the catalytic performances of phosphorus doped Cu-based catalysts for acetylene hydrochlorination at 140 ºC and GHSV (C_2H_2) of 180 h^{-1}. Introducing P into the catalyst significantly increased the activity compared

to monocomponent Cu (Fig. 1). And the $Cu_2P_2O_7$/SAC used for comparison also enhances the conversion but the conversion is lower than CuP/SAC catalysts, which indicates that the increase of conversion is not simply attributed to the formation of cupric pyrophosphate. Phosphoric acid-modified Cu/SAC catalysts showed volcano-type catalytic behavior in terms of the conversion of catalysts. Along with the phosphorus doping, the conversion of C_2H_2 increased and was maximized on the 2.5CuP/SAC catalyst which reached 72.4%. But further increase in the phosphorus loading led to a decrease in the conversion. As before, both Cu/SAC and CuP/SAC had very high selectivity to VCM in acetylene hydrochlorination (Table 2).

Table 2 Hydrochlorination performance of catalysts[a]

Catalyst	S_{VC}/%
Cu/SAC	99.6
$Cu_2P_2O_7$/SAC	99.0
0.5CuP/SAC	99.7
1CuP/SAC	99.7
2.5CuP/SAC	99.8
4CuP/SAC	99.5
6CuP/SAC	99.6

[a]Reaction conditions: T=140 ºC, n(HCl)/n(C_2H_2) = 1.15, GHSV (C_2H_2)=180 h^{-1}

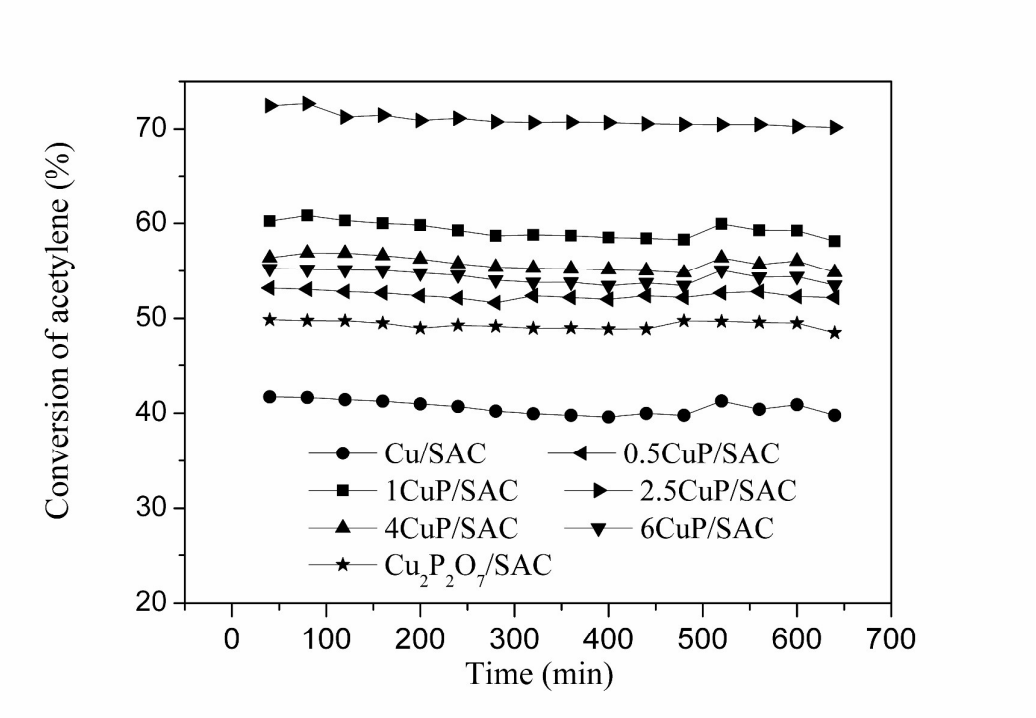

Fig. 2 The acetylene conversion over CuP catalysts; Reaction conditions: Temperature = 140 ºC, GHSV (C_2H_2) = 180 h^{-1}, n(HCl)/n(C_2H_2) = 1.15

Besides, we selected the unmodified Cu/SAC catalysts and the optimal 2.5CuP/SAC catalysts to investigate the stability after 100 h reaction under the condition of GHSV (C_2H_2) = 30 h^{-1}, n(HCl)/n(C_2H_2) = 1.15, T = 140 °C. The GHSV (C_2H_2) applied in industrial practice is very low because of the development of hot spots and the need to maintain high acetylene conversion,[27] thus we chose GHSV (C_2H_2) = 30 h^{-1} in lab to investigate the stability of the catalysts corresponding to industrial process.

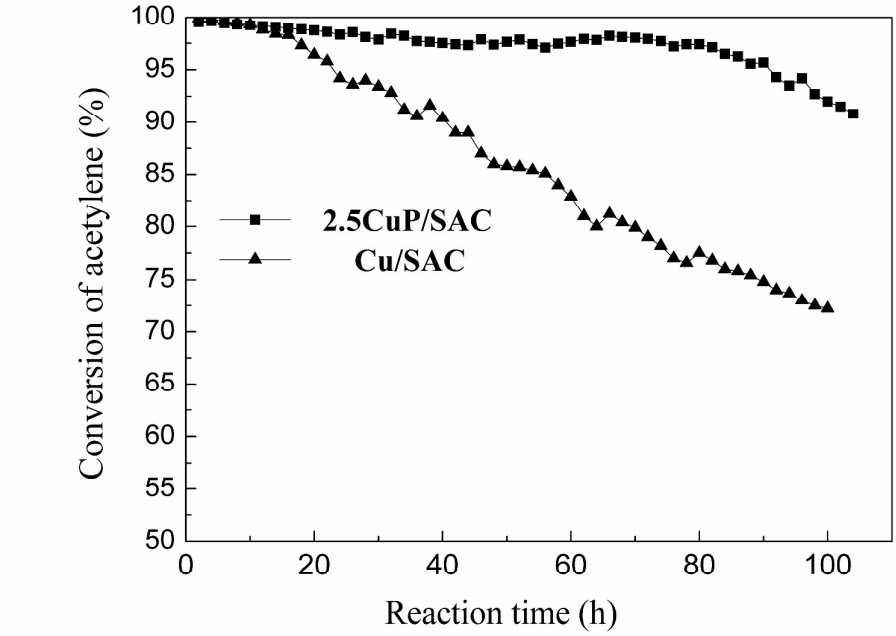

Fig. 3 Lifetime estimation of 2.5CuP/SAC and Cu/SAC catalysts; Reaction condition: GHSV $(C_2H_2) = 30\ h^{-1}$, T = 140 °C, $n(HCl)/n(C_2H_2) = 1.15$

The conversion of acetylene was tested and the result was shown in Fig. 3. It is indicated that the initial acetylene conversion for the two catalysts could reach 99%, which has meet the requirement of industrialization, but Cu/SAC catalyst was deactivated quickly after 24 h. However, compared to the Cu/SAC catalysts, after doping the phosphorus, the deactivation process was inhibited significantly because the acetylene conversion was still above 97.2% even after 82 hours reaction. But CuP/SAC catalysts deactivated rapidly in the subsequent reaction which suggested the catalysts also deactivated quickly compared to other catalysts although it has largely extended the lifetime of copper catalysts. So it is needed to investigate the deactivation mechanism of copper-based catalysts to offers the theoretical basement for later modification.

Characterization of catalysts

To understand the properties of catalyst samples, the effects of phosphoric acid treatment on the catalysts of Cu/SAC and the activation and deactivation mechanism of the catalysts, the original Cu/SAC and the modified CuP/SAC catalysts were characterized by BET, XRD, TEM, TPR, ICP, N_2O pulse titration, TG and XPS. To enable a clear discussion, both fresh and used catalysts were characterized, and the related results were displayed together.

Structural study of the catalysts

Table 3 lists the specific surface areas, total pore volumes and pore diameters of the fresh and used Cu/SAC and CuP/SAC catalysts (after 500 min). Due to the large number of micro-pores in the SAC surface, the N_2 adsorption-desorption isotherm of all of the catalysts belongs to type-I adsorption isotherms. As listed in Table 3, the specific surface areas and total pore volumes of the supports decrease after loading the active components. This result may be caused by the phenomenon called the dilution effect, in which the loading of the active components decrease the ratio of the carriers in the catalysts. When the loading increases, the dilution effect becomes more significant.[28] On the other hand, it may be also caused by the filling or blocking of the active components into the carrier pores. Once the loadings of active components increase, more pores of the carrier are filled or blocked by the active species, leading to a decrease of the BET surface area and the total pore volume. We can also see from the Tab. 3, after the reaction, the surface area of Cu/SAC catalyst declines from 674 $m^2 \cdot g^{-1}$ to 568 $m^2 \cdot g^{-1}$ (15.8% reduction), and meantime the total pore volume

reduces from 0.42 $cm^3 \cdot g^{-1}$ to 0.29 $cm^3 \cdot g^{-1}$ (30% reduction), which may be mainly due to the carbon deposition.

The doping of phosphorus into the Cu/SAC catalysts results in the change of surface area and total pore volume of catalysts. Cu/P ratios higher than 2.5 slightly influence the surface area and total pore volume, whereas further increasing phosphorus could result in a huge decline in both surface area and total pore volume. Phosphoric oxide, which was introduced by impregnation, was assumed to be likely to cover the Cu/SAC surface and plug channels or pores, resulting in a decrease of internal surface areas. Similarly, after the reaction, the surface area of 2.5CuP/SAC catalyst declines to 597 $m^2 \cdot g^{-1}$ (11.9%), and total pore volume reduces to 0.30 $cm^3 \cdot g^{-1}$ (11.9%). Thus, for the used CuP/SAC, the decrease in the surface area and total pore volume is smaller than those of the used Cu/SAC catalysts, indicating that the phosphoric acid treatment of catalysts can influence the deactivation of the catalysts in the acetylene hydrochlorination reaction by generating a significant variation in the structure of the used catalysts.

Table 3 Structural properties of catalysts

catalyst	S_{BET} ($m^2 \cdot g^{-1}$)		V_{pore} ($cm^3 \cdot g^{-1}$) Total pore volume		D_{pore}(nm) Pore diameter	
	fresh	used	fresh	used	fresh	Used
SAC	1012	--------	0.53	--------	1.92	--------
Cu /SAC (15%)	674	568	0.42	0.29	1.91	1.91
0.5CuP/SAC (15%)	657	572	0.38	0.31	1.91	1.91

1CuP/SAC (15%)	662	579	0.35	0.31	1.92	1.92
2.5CuP/SAC (15%)	678	597	0.34	0.30	1.92	1.92
4CuP/SAC (15%)	674	590	0.36	0.31	1.91	1.91
6CuP/SAC (15%)	670	588	0.38	0.33	1.92	1.92

Effect of the phosphorus on copper catalyst before and after reaction

Fig. 4 shows the XRD patterns of the fresh and used (after 500 min) Cu/SAC and phosphorus modified Cu/SAC catalysts. As shown in Fig. 4a, for the SAC support, there are two main diffraction peaks at around 25° and 43°, which are assigned to the (0 0 2) and (1 0 1) diffraction of the carbon, respectively.[29] Besides, introduction of phosphorus into Cu/SAC catalysts did not significantly change the crystal structure of the catalysts, meantime there had no other peaks detected both in Cu/SAC and CuP/SAC catalysts. Thus, it is worthwhile to note that active copper species disperse very well both in Cu/SAC and CuP/SAC catalysts as evidenced by no active copper species peaks found in XRD pattern because of the detect limitation of XRD.

Fig. 4b shows the XRD patterns of the fresh and used Cu/SAC and 2.5CuP/SAC catalysts. For Cu/SAC catalyst, diffraction peaks at 2θ of 16°, 17°, 32° and 40° for the copper atacamite ($Cu_2Cl(OH)_3$) became detectable based on the JCPDS file data[30] after reaction due to the agglomeration of copper atacamite species ($Cu_2Cl(OH)_3$). However, copper atacamite species have no activity in acetylene chlorination, because it has crystalline state of cupric compounds and will occupy the active sites

of the catalysts on the contrary. However, over the 2.5CuP/SAC catalyst, there have no sharp peaks before and after reaction, which suggests a good dispersion of the active copper sites before and after reaction. The XRD patterns of the used catalysts indicate that phosphorus-modified catalysts could suppress the agglomeration of the copper atacamite and promote the dispersion of copper species, which is in good agreement with the results of reaction lifetime. Thus, doping phosphorus can largely extend the lifetime of the catalysts.

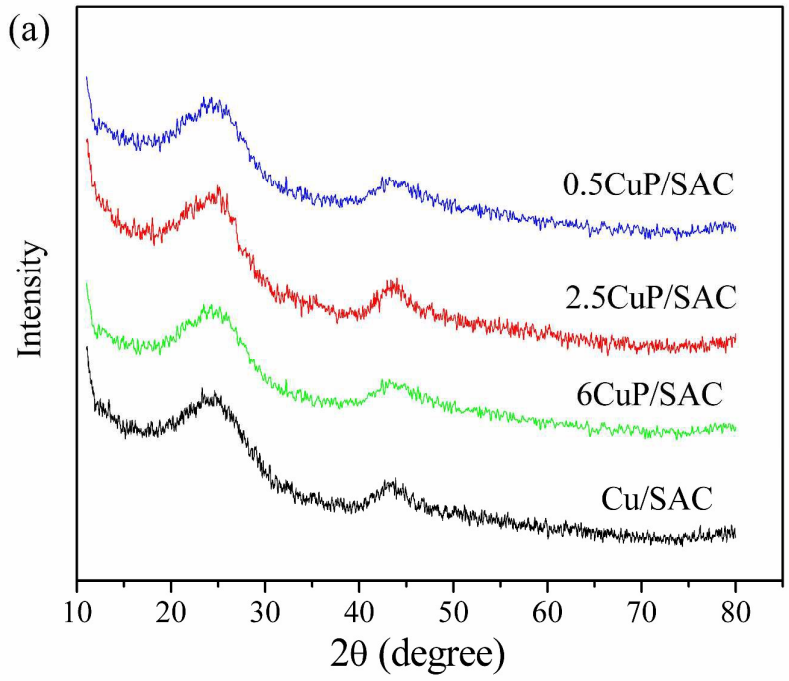

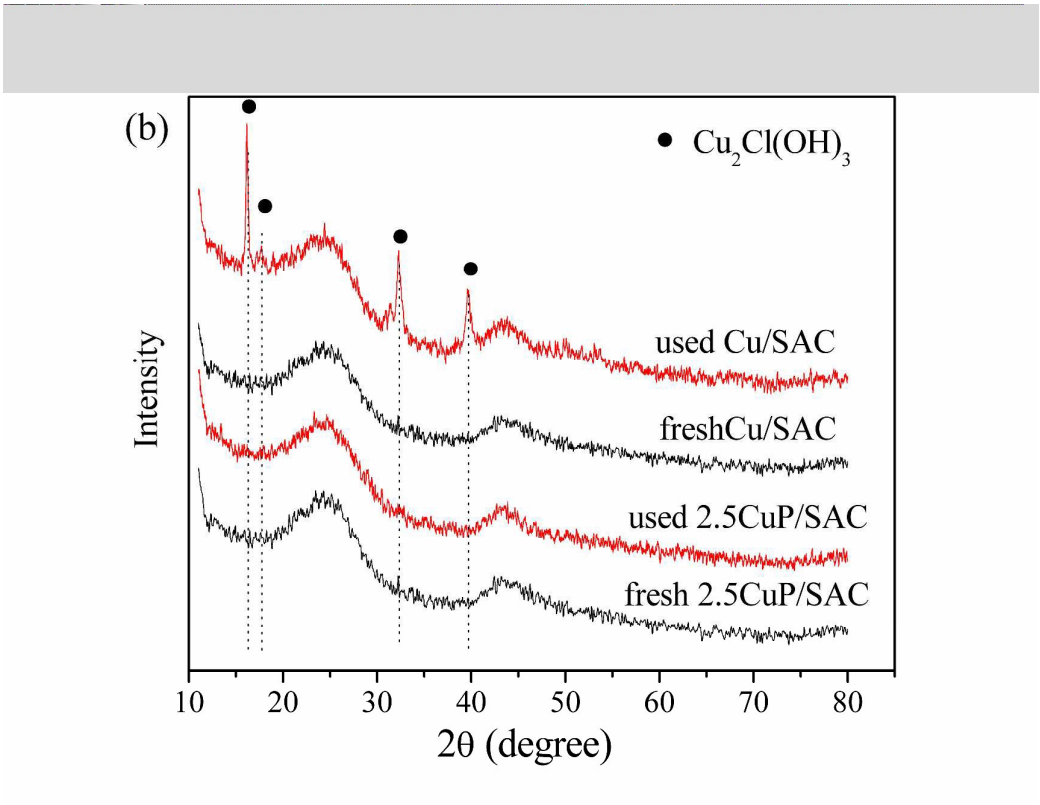

Fig. 4 XRD patterns of (a) the CuP/SAC catalysts; (b) fresh and used catalysts

TEM analysis was used to give a detailed image of copper species conditions, and it was considered a suitable method to give us an exact conclusion. It was expected that doping phosphorus may improve the distribution of copper species on the surface of activated carbon. Fig. 5 shows TEM images of the fresh and used Cu/SAC (Fig. 5 a and c) and 2.5CuP/SAC (Fig. 5 b and d) catalysts after 500 min reaction. It is apparent that the copper species were distributed uniformly on the support. The black particles attributed to Cu species suggested that these Cu nanoparticles became smaller after doping phosphorus on the catalysts. And the statistical results based on TEM images showed that the average copper particle size of fresh Cu/SAC and 2.5CuP/SAC catalysts is about 9.4 nm and 6.9 nm, respectively. Thus, TEM images of the fresh catalysts indicated that phosphorus-modified catalysts could make the

copper species better disperse on support. In addition, for the used catalysts after reaction, the particle size became larger, which suggested that the aggregation of copper species after reaction which can lead to the deactivation of catalysts. So it is indicated that phosphorus-modified catalysts may promote the dispersion of copper species and suppress the increase in Cu sizes.

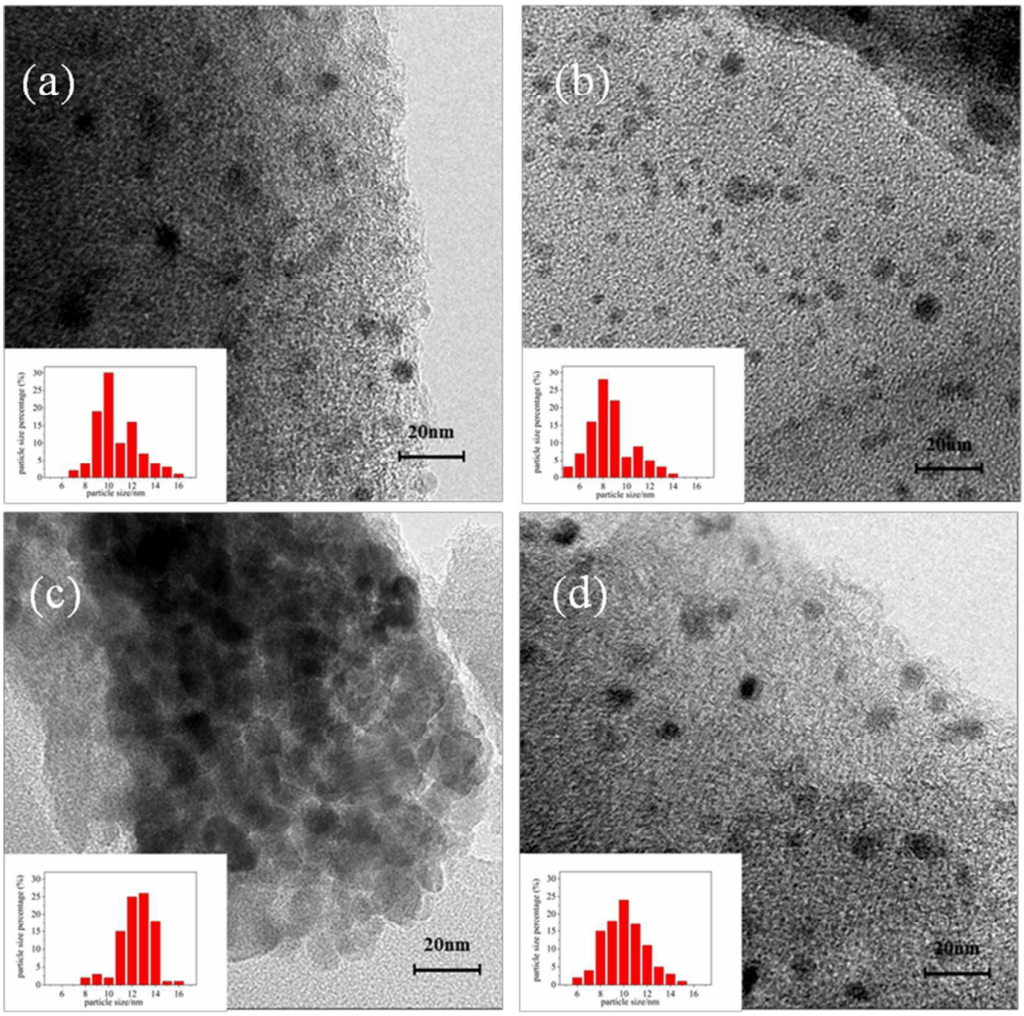

Fig. 5 TEM images of Cu/SAC (a, c) and 2.5CuP/SAC (b, d);before (a, b) and after (c, d) reaction

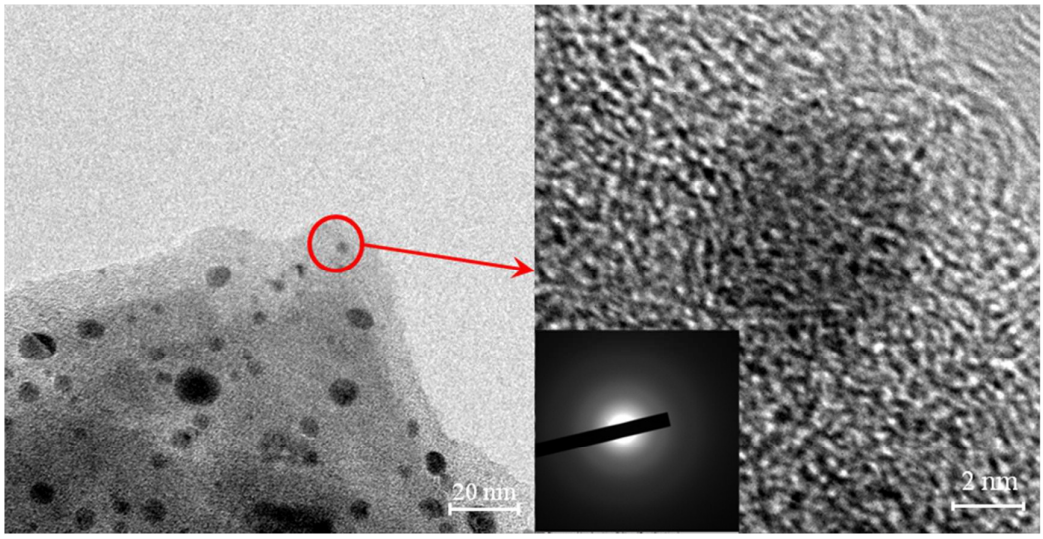

Fig. 6 High resolution TEM image and corresponding SAED patterns of 2.5CuP/SAC catalyst

We chose one place to analyze the nature of active components. HRTEM image and selected area electron diffraction of 2.5CuP/SAC catalysts given in Figure 6 reveals the nature of 2.5CuP/SAC NPs. The lattice fringes can not be seen in the spot (Fig. 6), indicating active components existed in the catalysts were not in the highly crystalline state and it might be highly amorphous in the catalysts. Further, selected area electron diffraction in the spot shows the active components are fully electron-diffraction amorphous as revealed by the broad and diffuse halos, and it is coherent with the results no lattice fringes was found in HR-TEM.

Further, XPS and XAES were carried out to elucidate the chemical states of copper chemical state of catalysts. The XPS and XAES spectra of fresh catalysts are shown in Fig. 7. As shown in Fig. 7a, Cu $2p_{3/2}$ and Cu $2p_{1/2}$, are accompanied with shake up peaks located at about 9 eV higher binding energy (BE) with respect to the main peaks, thus the presence of such satellites is typical of Cu^{2+} species.[31]. From the curve fitting, the peak at 932-935 eV are discerned into two peaks. The position of the first

main peak is at 934.6-934.2 eV, while the second small one is situated at 931.9-932.1 eV BE. The higher energy peak can be assigned to Cu^{2+}, while the lower energy peak could be related to Cu^{+} or Cu^{0} species.[32, 33] Thus, the results of Cu $2p_{3/2}$ XPS indicates that Cu^{2+} was the main active component in the catalysts.

The binding energy for Cu^{0} and Cu^{+} species is almost the same, and their difference depends on the XAES spectra.[34] Fig. 7b shows the curves in the Auger Cu LMM spectra. In the peak fit of Cu LMM, shown in Fig. 7b, there are one main peak at 916.4-916.6 eV (Cu^{+}) and one or two other peaks at 910.5 eV and 920.2 eV that represent different transitions states of the Cu LMM spectrum.[35] Thus, the Cu LMM transition showing only Cu^{+} species in all fresh catalyst samples. Hutchings *et al* [8-14] studied that Cu^{2+} and Cu^{+} metal components both have activity for hydrochlorination reaction and the initial activity of Cu-based catalysts was almost same: $Cu^{2+} \approx Cu^{+}$.

From the deconvolution results of Cu $2p_{3/2}$ XPS, the molar ratio of surface Cu^{2+} and Cu^{+} were measured by the peak area. Molar ratio Cu^{2+}/Cu^{+} was increased as the ratio Cu/P decreased (shown in Table 4), and 2.5CuP/SAC catalysts achieved the highest molar ratio of surface Cu^{2+}/Cu^{+}. Consequently, in combination of the results of conversion of acetylene, the results of Cu $2p_{3/2}$ XPS indicates that Cu^{2+} acts as the primary active site in the mixed active components in the hydrochlorination reaction.

Besides, in Fig. 7c, the peak at 135.2 eV has a binding energy similar to that of P_2O_5 (135.2 eV).[36] As the Cu/P ratio decreases, the surface amount of phosphorus oxide increases remarkably according to the intensity of P 2p peaks.

The XPS and XAES spectra of used catalysts were shown in Fig. 8. In Fig. 8a, the

main peak at 934.3 eV is assigned to the state Cu^{2+} in the spinel, accompanied by the characteristic Cu^{2+} shakeup satellite peaks (940-945eV), suggesting Cu^{2+} is still the main component in the used catalysts. However, the area ratio of peak at 934.2 eV (Cu^{2+}) and 932.1 eV (Cu^{+} or Cu) decreased after reaction for both Cu/SAC and phosphorus modified Cu/SAC catalysts, which proved the active components were reduced after the reaction. Besides, in the Cu LMM XAES spectra of used catalysts (Fig. 8b), asymmetry and broad Auger kinetic energy were observed and deconvoluted into two symmetrical peaks located at around 918.6 and 916.6 eV,[37] corresponding to Cu^{0} and Cu^{+}, respectively. It is obviously that Cu^{0} was generated after the reaction, which can not be seen in fresh catalyst samples shown in Fig. 7b. Corresponding to the results of the catalysts conversion, therefore, the reduction of active components is also the reason for the deactivation of catalysts. Meantime in the the Cu LMM XAES spectra as shown in Fig. 8b, the area peak at 918.6 eV (Cu) accounts for higher percentage for Cu/SAC catalyst, thus it is important to note that addition of phosphorus can retard the reduction of the active componnets (Cu^{2+}/Cu^{+}) to Cu^{0} to a certain extent.

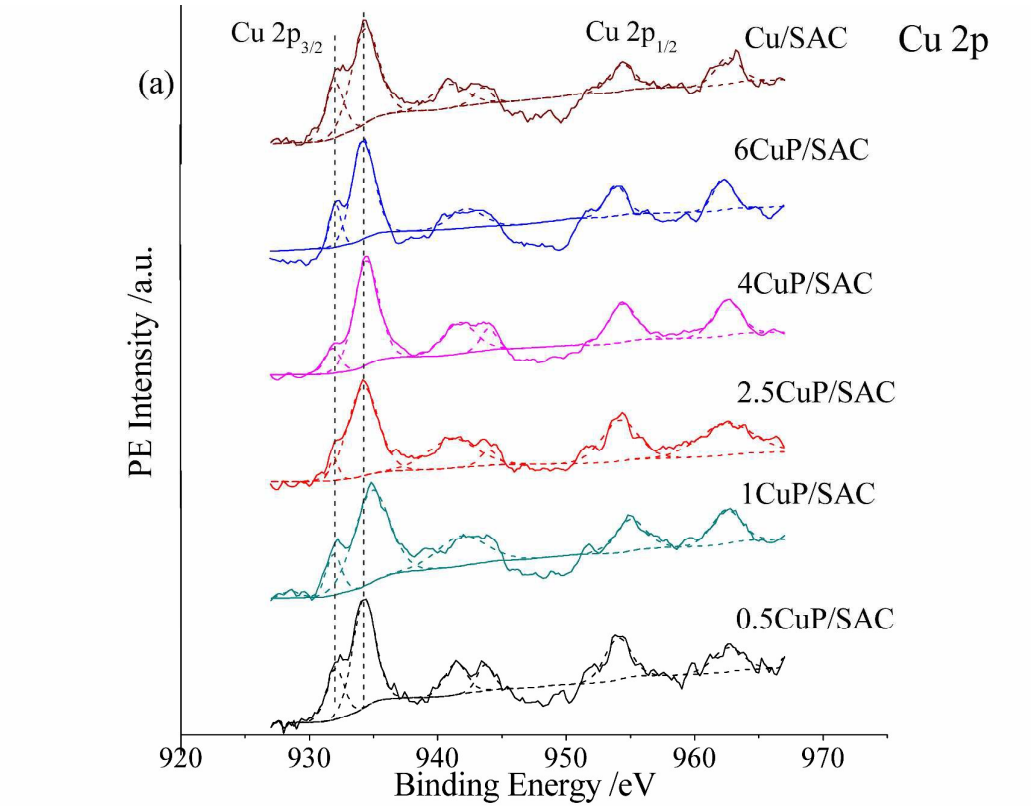

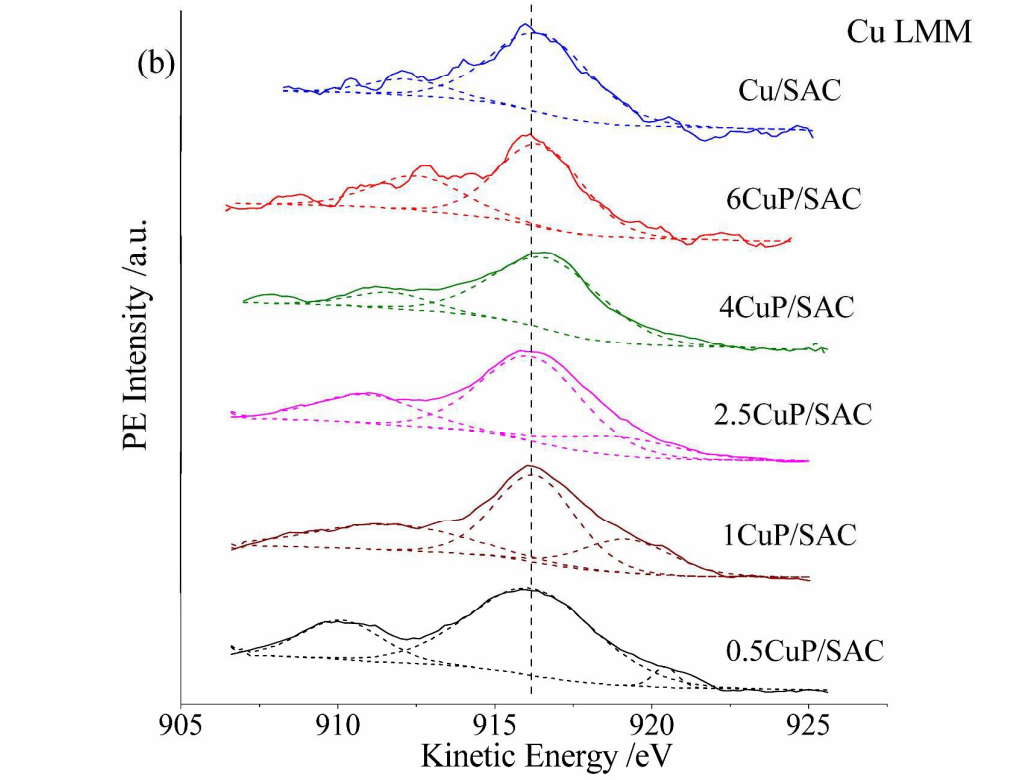

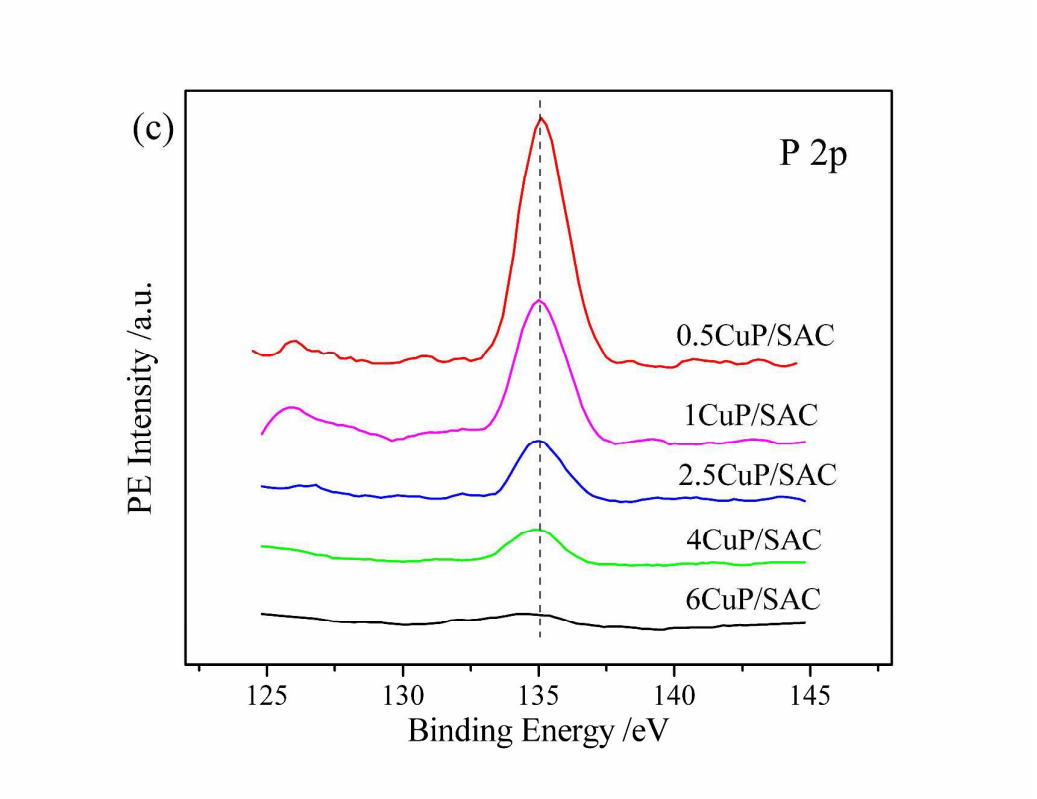

Fig. 7 (a) Copper 2p XPS spectra of samples; (b) Cu LMM Auger spectra (c) P 2p XPS spectra of samples

Table 4 Surface Cu component of catalysts based on Cu $2p_{3/2}$ XPS

Catalysts	BE of Cu $2p_{3/2}$ (eV)		$A_{Cu^{2+}/Cu^{+}}$
	Cu^{2+}	Cu^{+}	
Cu/SAC	934.3	932.1	1.28
0.5Cu/SAC	934.3	932.0	1.64
1Cu/SAC	934.2	932.0	3.32
2.5Cu/SAC	934.4	931.9	5.58
4Cu/SAC	934.6	932.0	3.70
6Cu/SAC	934.3	932.0	2.37

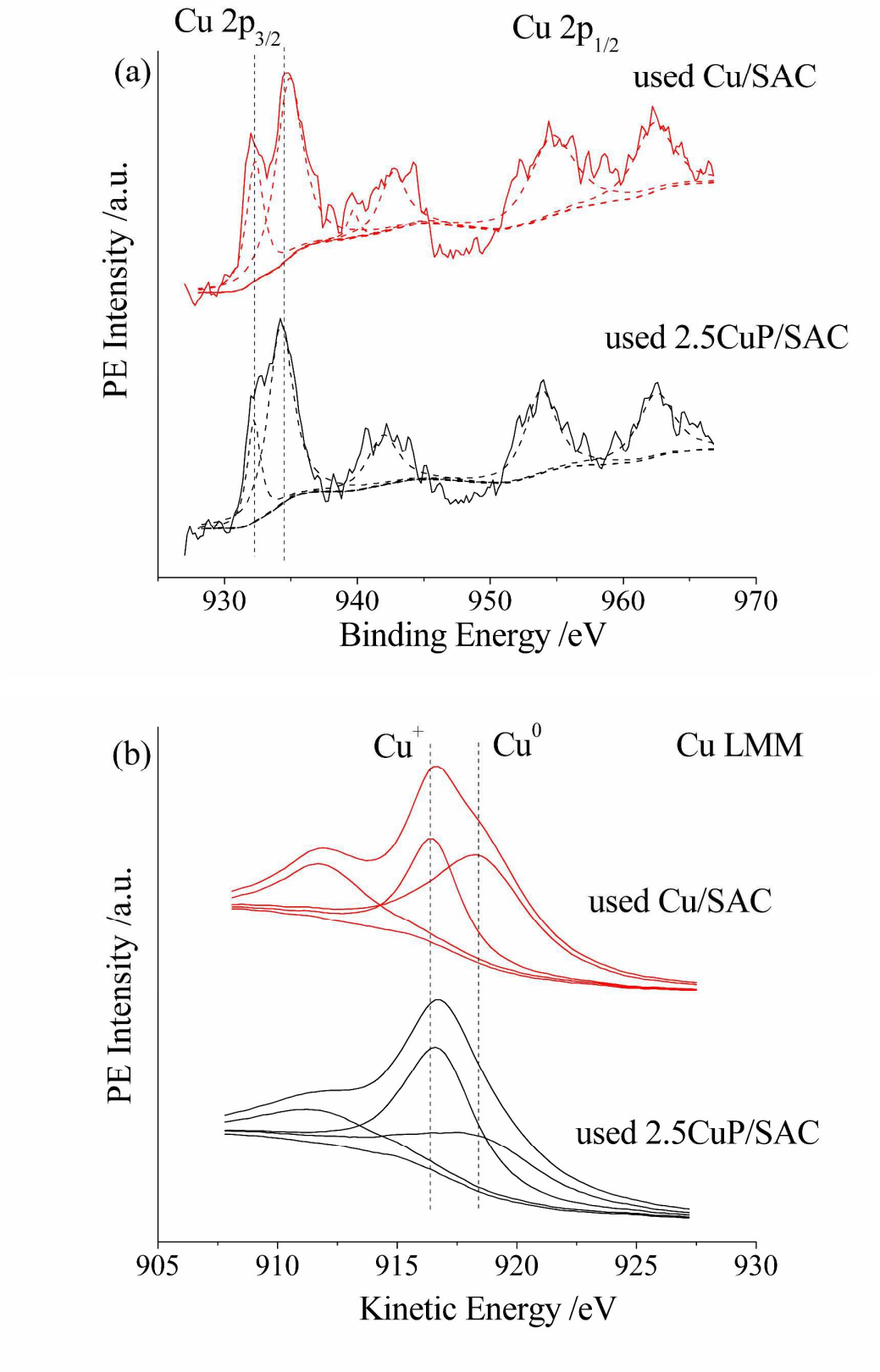

Fig. 8 (a) Copper 2p XPS spectra of samples; (b) Cu LMM Auger spectra of samples

Fig. 9 displays the TPR profiles of the Cu/SAC, 0.5CuP/SAC, 2.5CuP/SAC 4CuP/SAC, 6CuP/SAC catalysts. For the Cu/SAC sample, besides the main reduction peak at 285 ºC, there was a shoulder peak at 337 ºC, which was vanished for phosphorus modified Cu/SAC catalyst. This shoulder peak is assigned to the reduction of large Cu^{2+} particles to metallic Cu and the assignment is in compliance with the fact that the reduction of bulk Cu^{2+} metal components usually occurs at 270-330 ºC [38-40], which is consistent with the TEM characterization.

For the CuP/SAC, the peak around 340 ºC are attributed to the reduction of Cu^{2+} to Cu.41 And another small peak around 400 ºC also appear attributed to the reduction of Cu^{+} to Cu^{0}.[42] Besides, as shown in Fig. 9, the peak has the tendency to be sharp with increasing phosphorus content, indicating that adding phosphorus could increase the dispersion of copper species. In Fig. 9, for CuP/SAC catalysts, the reduction peaks shifts to higher temperatures with the increase in the phosphorus loading, which was probably due to the chemical interaction between the basic copper species and the carbon support. Furthermore, the reduction peak is found to increase steadily at relative suitable phosphorus content, maximize on the 2.5CuP/SAC catalysts, and decline with continuous increase in the phosphorus content, which is also accord with the results of conversion of acetylene hydrochlorination.

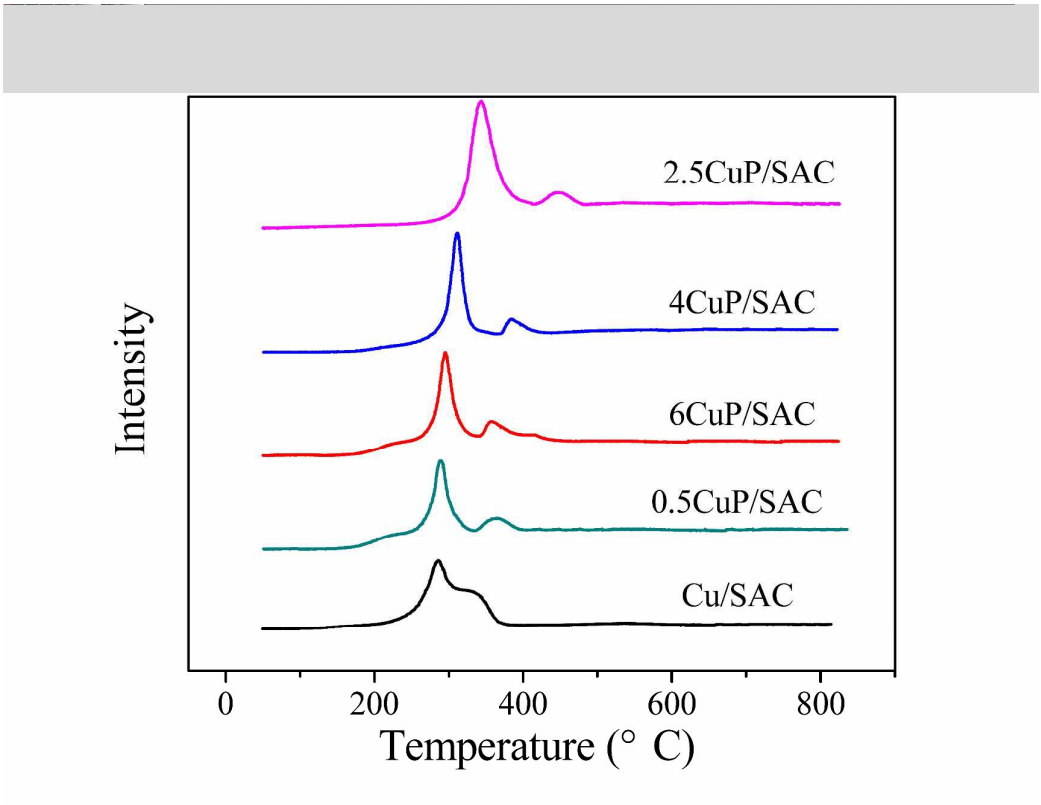

Fig. 9 H_2-TPR profiles of the CuP/SAC catalysts

Copper dispersion are crucial factors determining catalytic performance of copper-based catalysts. It is known that the dispersion of Cu elements can be measured by the adsorption and decomposition of N_2O using the pulse titration method.

As listed in Table 5, phosphorus doping induced noticeable enhancement of copper dispersion. The copper dispersion is 36.8% for the original Cu/SAC. For the phosphorus modified Cu/SAC catalysts, the highest dispersion achieved in 2.5CuP/SAC (48.8%). Corresponding to the TEM images and results of reaction, these data suggest that, after doping phosphorus on the catalysts, the dispersion of copper was improved.

Table 5 Estimated copper dispersion in the catalysts

Catalysts	Cu loading (wt%)[a]	Cu dispersion (%)[b]
Cu/SAC	14.7	36.8
0.5CuP/SAC	14.9	41.7
1CuP/SAC	14.9	44.2
2.5CuP/SAC	14.8	48.8
4CuP/SAC	14.6	47.5
6CuP/SAC	14.8	46.9

a Determined by ICP-AES

b Cu determined by N_2O titration method

Cu/SAC catalysts modified with suitable amounts of phosphorus display enhanced activity of acetylene hydrochlorination. Additionally, there is no significant textual structure change in the pore structures after doping phosphorus discussed before. So we deduce that the structures of samples are not the main reasons affecting the conversion of the reaction. As characterized before, the copper dispersion of the catalysts has the main influence on the conversion of acetylene hydrochlorination. Catalysts modified by suitable amounts of phosphorus have significantly improved the dispersion of copper species, whereas further adding phosphorus in the catalysts may cover the active sites of the catalyst. Thus, there was a strong correlation between the VCM yield and the copper dispersion on the catalyst. As discussed before, the 2.5Cu/SAC catalyst gets the highest VCM yield, which indicates that high copper dispersion and small copper components size are important to the process of the acetylene hydrochlorination to VCM.

Based on our results and reference discussed before, a summary schematic model of influence mechanism of phosphorus doping on Cu-based catalysts was provided and shown in Fig. 10. Without phosphorous doping, the copper chloride is apt to

aggregate on the surface of the support because of the week interaction between the copper chloride and support, which was evidenced by the big particle size in fresh and used Cu/SAC catalyst. With the adding of phosphorus into the catalyst, generated defects promote the dispersion of copper species leading to the decrease of particle size. The interaction between the copper chloride and phosphorus oxide also strengthen. However, excessively high phosphorus oxide adding can lead to covering the active sites on the surface and blocking the internal surface areas. Thus, there exists an optimal amount of phosphorus doping on the catalysts.

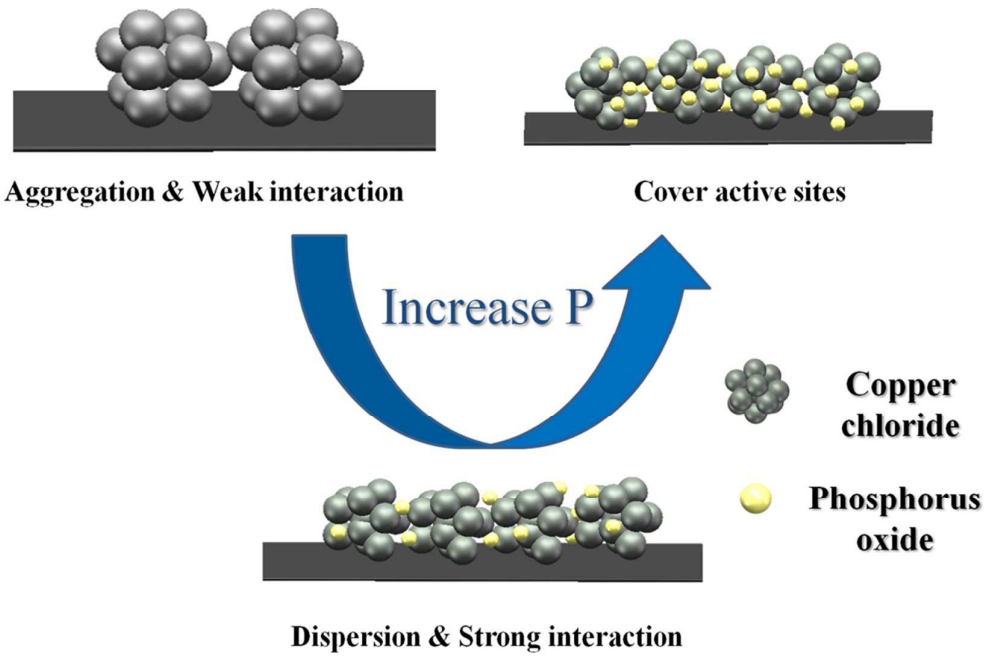

Fig. 10 Schematic model of the catalysts with increasing phosphorus

Carbon deposition and loss of the active component

Thermo Gravimetric (TG) analysis was used to evaluate the deposition on the used Cu/SAC and phosphorus modified Cu/SAC catalysts. As shown in Figure 11, for used Cu/SAC catalyst, the slight weight loss before 150 ºC is due to the desiccation

of adsorbed water. The obvious weight loss in the temperature range of 150-350 ºC is associated with the burning of carbon deposited on the catalyst surface and the rapid weight loss above 350 ºC is caused by the burning of SAC support. It is the weight loss in the range of 150-350 ºC that reflects the amount of coking deposition on the catalyst surface. It can be seen that the weight loss of the used Cu/SAC is 7% in the temperature range of 150-350 ºC, while it is 3% for the fresh Cu/SAC. Consequently the carbon deposition of the catalyst surface is approximately 4% for the used Cu/SAC in Table 6, according to the coke deposition calculation for the same temperature interval.

In the case of 2.5CuP/SAC catalyst, the weight loss in the temperature range of 150-350 ºC of the used and fresh catalysts was 7.5% and 5.5%, respectively, which suggest the carbon deposition of the catalyst surface is approximately 2% (Table 6). It can be concluded that the deactivation of both Cu/SAC and CuP/SAC catalysts is somewhat caused by carbon deposition, and the addition of phosphorus can inhibit carbon deposition effectively, which is in accord of the lifetime and characterization of the catalyst. The amount of carbon deposition on the catalysts was determined based on the calculation method described above, and the results are listed in Table 6. For the phosphorus modified catalysts, the carbon deposition was similarly determined to be 2.4% for 4CuP/SAC, 2.6% for the used 0.5CuP/SAC and 1CuP/SAC and 2.9% for the used 6CuP/SAC catalysts. And the carbon deposition also tends to decrease with increasing phosphorus content. This further indicates that the phosphorus modified treatment can influence the coking deposition on the surface

of Cu-based catalysts. The effect of P addition on inhibition of carbon deposition is consistent with the characterizations and results discussed before.

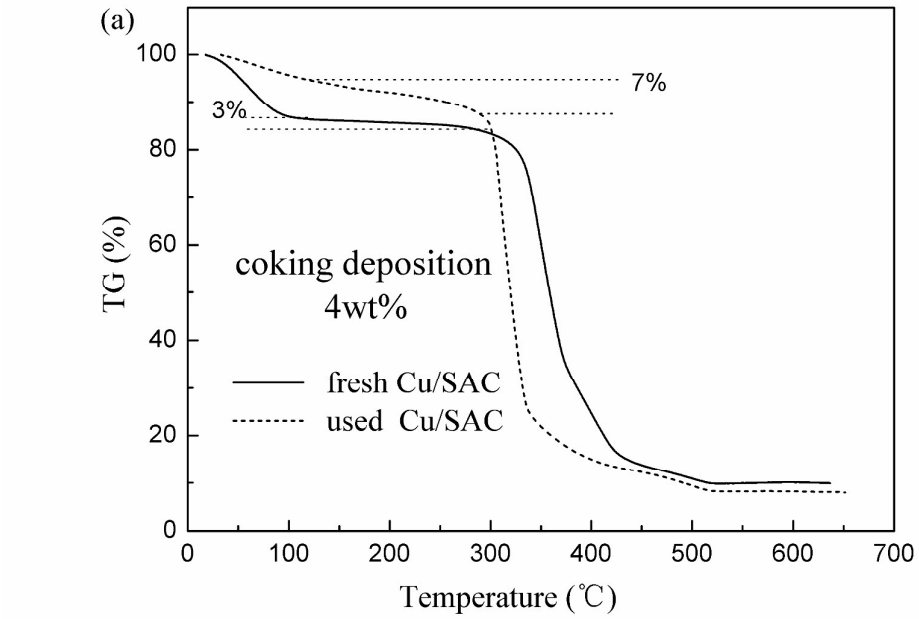

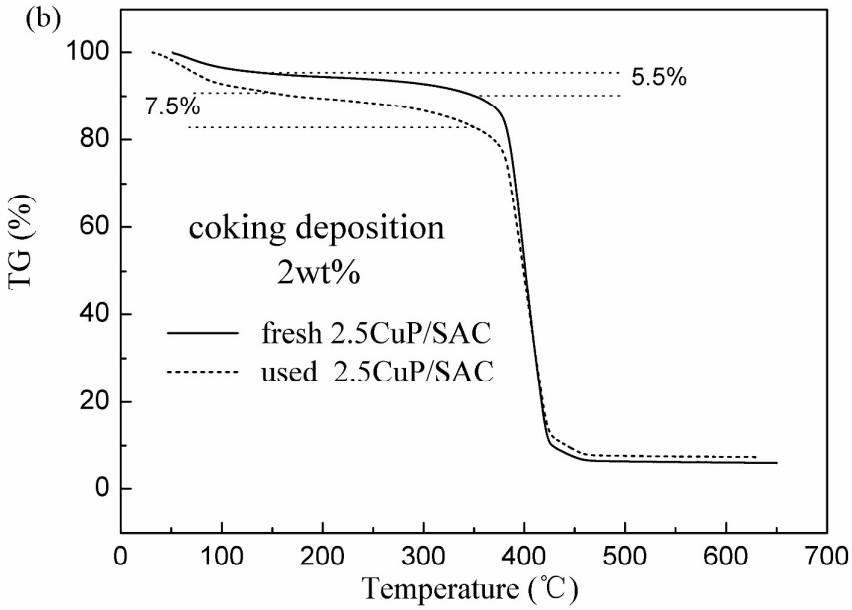

Fig. 11 TG cures of fresh and used 2.5CuP/SAC catalysts

Table 6 Carbon deposition of Cu-based catalysts

Catalysts	Amount of carbon deposition (%)
Cu/SAC	4.0
0.5Cu/SAC	2.7
1Cu/SAC	2.7
2.5Cu/SAC	2.0
4Cu/SAC	2.4
6Cu/SAC	2.9

In addition, the total Cu content in the fresh and used catalysts was also measured by ICP. Before the ICP characterization, the used catalysts were calcined coke prior to the ICP measurements in order to exclude the influence of carbon deposition. As listed in Table 7, total Cu content in the used catalyst is less than that of the fresh catalysts. For the catalyst Cu/SAC, the loss ratio of Cu is 8.16% after 100 h reaction while for the CuP/SAC catalyst the loss ratio is 5.41%, indicating that the catalyst is much stable after doping phosphorus. It can also be concluded that the loss of the active components is one of the reasons leading to the deactivation of the catalysts, but it isn't the main reasons for deactivation of the catalyst because of not much quantity of active component losing.

Table 7 ICP of Cu/SAC and CuP/SAC samples

Catalysts	Total Cu (wt%)		Loss ratio of Cu (%)
	Fresh	Used	
Cu/SAC	14.7	13.5	8.16
2.5CuP/SAC	14.8	14.0	5.41

Conclusions

In the hydrochlorination of acetylene with carbon-supported $CuCl_2$ catalysts, it was

observed that Cu-based catalysts had relative higher activity. The conversion of the catalysts varies with different copper loading, and when the Cu loading reaches 15wt%，the catalyst achieves highest conversion. And the phosphorus doped on Cu/SAC catalysts has an important effect on their catalytic performance in the hydrochlorination acetylene reaction. After an optimal amount of phosphorus was added into the catalysts, an increase in dispersion of copper species and a decrease in copper particle size were observed. On the other hand, excessive introduction of the phosphorus could make the aggregation of the active oxide and cover catalyst surface, leading to decreases of catalytic performance. Besides, doping phosphorus could possibly restrain the aggregation of copper nanoparticles, resulting in excellent catalytic stability. The 2.5CuP/C catalyst was shown to be deactivated after 82 h extending the age of the catalysts compared to the Cu/SAC. The loss of active components, the aggregation of active copper species, the reduction of the active components and deposition of carbonaceous material on the catalyst is the reasons account for the deactivation of catalysts in acetylene hydrochlorination.

Acknowledge

We gratefully acknowledge financial support by the National Basic Research Program of China (973 Program) (Grant No: 2012CB720302) and the Program for Changjiang Scholars and Innovative Research Teams in Universities (IRT0936).

References

1. G. J. Hutchings and D. T. Grady, *Applied Catalysis*, 1985, **17**, 155-160.
2. G. J. Hutchings and D. T. Grady, *Applied Catalysis*, 1985, **16**, 411-415.
3. X. Wei, H. Shi, W. Qian, G. Luo, Y. Jin and F. Wei, *Industrial & Engineering Chemistry*, 2009, **48**, 128-133.

4. J. Zhang, N. Liu, W. Li and B. Dai, *Frontiers of Chemical Science and Engineering*, 2011, **5**, 514-520.
5. D. M. Smith, P. M. Walsh and T. L. Slager, *Journal of Catalysis*, 1968, **11**, 113-130.
6. A. K. Ghosh and J. B. Agnew, *Industrial & Engineering Chemistry Product Research and Development*, 1985, **24**, 152-159.
7. J. B. Agnew and H. S. Shankar, *Industrial & Engineering Chemistry Product Research and Development*, 1986, **25**, 19-22.
8. G. J. Hutchings, *Journal of Catalysis*, 1985, **96**, 292-295.
9. B. Nkosi, N. J. Coville and G. J. Hutchings, *Journal of the American Chemical Society, Chemical Communications*, 1988, **1**, 71.
10. B. Nkosi, M. D. Adams, N. J. Coville and G. J. Hutchings, *Journal of Catalysis*, 1991, **128**, 378-386.
11. B. Nkosi, N. J. Coville, G. J. Hutchings, M. D. Adams, J. Friedl and F. E. Wagner, *Journal of Catalysis*, 1991, **128**, 366-377.
12. G. J. Hutchings and M. Haruta, *Applied Catalysis A: General*, 2005, **291**, 2-5.
13. M. Conte, A. F. Carley and G. J. Hutchings, *Catalysis Letters*, 2008, **124**, 165-167.
14. G. J. Hutchings, *Topics in catalysis*, 2008, **48**, 55-59.
15. M. Conte, A. Carley, G. Attard, A. Herzing, C. Kiely and G. Hutchings, *Journal of Catalysis*, 2008, **257**, 190-198.
16. H. Kobayashi, N. T and C. Minochi, *Journal of Catalysis*, 1981, **69**, 487.
17. K. Zhou, J. Si, J. Jia, J. Huang, J. Zhou, G. Luo and F. Wei, *RSC Advances*, 2014, **4**, 7766.
18. D. von Deak, E. J. Biddinger, K. A. Luthman and U. S. Ozkan, *Carbon*, 2010, **48**, 3637-3639.
19. K. Chizari, A. Deneuve, O. Ersen, I. Florea, Y. Liu, D. Edouard, I. Janowska, D. Begin and C. Pham-Huu, *ChemSusChem*, 2012, **5**, 102-108.
20. R. Li, Z. Wei, X. Gou and W. Xu, *RSC Advances*, 2013, **3**, 9978.
21. J. Wu, Z. Yang, X. Li, Q. Sun, C. Jin, P. Strasser and R. Yang, *Journal of Materials Chemistry A*, 2013, **1**, 9889.
22. Z. Liu, F. Peng, H. Wang, H. Yu, J. Tan and L. Zhu, *Catalysis Communications*, 2011, **16**, 35-38.
23. Z. Liu, F. Peng, H. Wang, H. Yu, W. Zheng and J. Yang, *Angewandte Chemie International Edition*, 2011, **50**, 3257-3261.
24. Z. Chen, D. H, T. Haisheng, S. Ryan and Z. Chen, *Journal of the American Chemical Society*, 2009, **113**, 21008-21013.
25. Y. Hu, J. Zhu, Q. Lv, C. Liu, Q. Li and W. Xing, *Electrochimica Acta*, 2015, **155**, 335-340.
26. A. Dandekar and M. A. Vannice, *Journal of Catalysis*, 1998, **178**, 621-639.
27. H. Zhang, B. Dai, W. Li, X. Wang, J. Zhang, M. Zhu and J. Gu, *Journal of Catalysis*, 2014, **316**, 141-148.
28. H. Zhang, B. Dai, X. Wang, W. Li, Y. Han, J. Gu and J. Zhang, *Green Chemistry*, 2013, **15**, 829.
29. L. Li, Z. H. Zhu, Z. F. Yan, G. Q. Lu and L. Rintoul, *Applied Catalysis A: General*, 2007, **320**, 166-172.
30. A. J. Rouco, *Journal of Catalysis*, 1995, **157**, 380-387.
31. F. Raimondi, K. Geissler, J. Wambach and A. Wokaun, *Applied Surface Science*, 2002, **189**, 59-71.

32. F. Severino, J. L. Brito, J. Laine, J. L. G. Fierro and A. L. o. Agudo, *Journal of Catalysis*, 1998, **177**, 82-95.
33. K. L. Deutsch and B. H. Shanks, *Journal of Catalysis*, 2012, **285**, 235-241.
34. J. Gong, H. Yue, Y. Zhao, S. Zhao, L. Zhao, J. Lv, S. Wang and X. Ma, *Journal of the American Chemical Society*, 2012, **134**, 13922-13925.
35. P. Dubot, D. Jousset, V. Pinet, F. Pellerin and J. P. Langeron, *Surface and Interface Analysis*, 1988, **12**, 99-104.
36. S. Baunack, S. Oswald and D. Scharnweber, *Surface and Interface Analysis*, 1998, **26**, 471-479.
37. I. Platzman, R. Brener, H. Haick and R. Tannenbaum, *Journal of the American Chemical Society*, 2008, **112**, 1101-1108.
38. M. Shimokawabe, N. Takezawa and H. Kobayashi, *Applied Catalysis*, 1982, **2**, 379-387.
39. G.D. Lei, B. T. Carvill and W. M. H. Sachtler, *Applied Catalysis A: General*, 1996, **142**, 347-359.
40. F. W. Chang, H. C. Yang, L. S. Roselin and W. Y. Kuo, *Applied Catalysis A: General*, 2006, **304**, 30-39.
41. F. Gao, E. D. Walter, N. M. Washton, J. Szanyi and C. H. F. Peden, *Applied Catalysis B: Environmental*, 2015, **162**, 501-514.
42. C. S. Polster, H. Nair and C. D. Baertsch, *Journal of Catalysis*, 2009, **266**, 308-319.

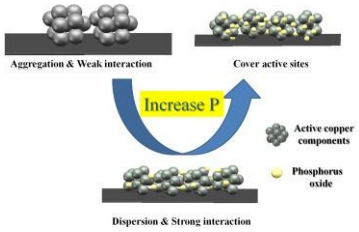

The phosphorus doping facilitates the dispersion of copper species, enhances the interaction between metal and support, and restrains the growth of copper components during acetylene hydrochlorination.